Densification of Supercritical Carbon Dioxide Accompanied by Droplet Formation When Passing the Widom Line

Vitaliy Pipich[1] and Dietmar Schwahn[2,*]
[1]Forschungszentrum Jülich GmbH, Jülich Centre for Neutron Science (JCNS) at Heinz Maier-Leibnitz Zentrum (MLZ), Lichtenbergstraße 1, D-85748 Garching, Germany
[2]Technische Universität München, Forschungs-Neutronenquelle Heinz Maier-Leibnitz (FRM II), James-Franck-Straße 1, D-85748 Garching, Germany

(Received 20 November 2017; revised manuscript received 23 January 2018; published 5 April 2018)

Thermal density fluctuations of supercritical CO_2 were explored using small-angle neutron scattering (SANS), whose amplitude (susceptibility) and correlation length show the expected maximum at the Widom line. At low pressure, the susceptibility is in excellent agreement with the evaluated values on the basis of mass density measurements. At about 20 bar beyond the Widom line, SANS shows the formation of droplets accompanied by an enhanced number density of the supercritical fluid. The corresponding borderline is interpreted as a Frenkel line separating gas- and liquidlike regimes.

DOI: 10.1103/PhysRevLett.120.145701

Introduction.—Supercritical carbon dioxide (CO_2) is a relevant solvent in industrial application. It is classified as a "green" solvent because of its nontoxicity, chemical stability, and reusability [1]. Among many other studies there are extensive small-angle neutron scattering (SANS) experiments studying the solution properties of polymers in supercritical CO_2 [2]. This Letter presents a SANS study about supercritical CO_2, exploring thermal density fluctuations as a function of external pressure along an isothermal pathway.

The pressure-temperature plane of the CO_2 phase diagram is shown in Fig. 1. The gas-liquid and liquid-solid phase boundaries are plotted as bulky solid lines [3]. The coordinates of the critical point are $T_C = 31\,°C$ and $P_C = 73.8$ bar. Beyond the critical point, one has the supercritical fluid region. In classical thermodynamics, one learns that supercritical fluids represent a homogeneous phase, allowing a continuous transformation of the gas phase to the liquid phase without passing the first order phase transition line. Supercritical fluids, however, show more complex phase behavior, as has been shown quite recently in the context of the Widom and Frenkel lines [4,5]. The Widom line, plotted as dashed line, represents a continuation of the gas-liquid line beyond the critical point and is defined as the maximum of thermodynamic response functions. It does not represent a singularity and therefore no borderline of second order phase transition [6]. In our case, the Widom line is evaluated from the compressibility taken from [3] [see also Eq. (S-1) in the Supplemental Material [7]], as this parameter is measured in scattering experiments. The Frenkel line is defined as a borderline separating the two dynamically distinct phases of gas- and liquidlike behavior [4,8–10]. In the gas- and liquidlike regimes, the motion of molecules is purely diffusive and diffusive as well as solidlike vibrational, respectively. A similar borderline (Fisher-Widom line) was proposed by Fisher and Widom, defining gas- and liquidlike regimes on basis of the, respectively, monotonic and oscillatory asymptotic decay of the pair correlation function [11,12]. Three Frenkel lines are copied in Fig. 1, evaluated from

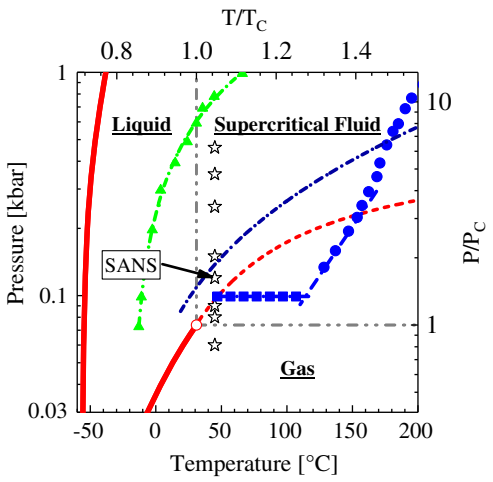

FIG. 1. Temperature-pressure plane of the CO_2 phase diagram. The bulky solid lines show the liquid-solid and gas-liquid phase boundaries and the critical point. The dashed line shows the Widom line derived from isothermal compressibility [3], whereas three Frenkel lines derived from MD simulations are depicted by dashed-dotted lines. The Frenkel line depicted with solid circles and squares was derived from isochoric heat capacity in [8], with triangles from the velocity autocorrelation function in [10], and with the purely dashed-dotted line on the basis of a Lennard-Jones fluid [Fig. 18(a) of [4]]. The positions of SANS measurement are shown by the open stars and the experimental Frenkel line is indicated by the arrow.

molecular dynamic (MD) simulation. The Frenkel line, depicted as solid squares and spheres, was determined on the basis of isochoric heat capacity (Figs. 4 and 8 in [8]), the dashed-dotted line was evaluated for a Lennard-Jones fluid [Fig. 18(a) in [4]], and the triangles on the basis of the velocity autocorrelation function [Fig. 2(a) in [10]].

The SANS experiments were performed at 45 °C and at pressure fields between 60 and 460 bar, i.e., at $T/T_C = 1.046$ and $P/P_C = 0.81$–6.23, shown by the open stars in Fig. 1, and determines the Widom line at 97 bar ($P/P_C = 1.31$) and the Frenkel line at about 120 bar ($P/P_C = 1.63$). The Frenkel line was identified from the formation of droplets and a number density larger than predicted from equation of state theories.

Experimental.—The SANS experiments were performed at KWS 1 operated by JCNS at MLZ (FRM II) in Garching at a sample-to-detector distance of 1.70 m and a few times at 7.70 m in order to reach smaller scattering angles [13]. The neutron wavelength was 5 Å with $\Delta\lambda/\lambda = 10\%$. The pressure cell was particularly designed for SANS experiments, with two sapphire windows allowing a 4 cm diameter area for neutrons to pass and a 0.4 cm thickness for the gas. This cell allows a pressure up to 500 bar. Temperature and pressure show an estimated absolute error of ± 1 K and ± 2 bar. The SANS data were corrected for background scattering and detector efficiency and calibrated in absolute units using a secondary standard.

Carbon dioxide (type 5.3) of purity better than 99.9993% was purchased from Linde AG (Munich, Germany). Relevant parameters of CO_2 for neutron scattering experiments are compiled in Supplemental Material Table SI [7]. The covolume of CO_2 molecules is related to the van der Waals parameter b being approximately four times larger than the molecular volume Ω (see for e.g., Chapter 10.3 in [14]). The coherent scattering length was determined from the values of carbon and oxygen given in [15], according to $b_{CO_2} = b_C + 2b_O$. The incoherent scattering $d\Sigma/d\Omega_{inc}$ is negligible (Supplemental Material Table SI).

Theoretical background.—Thermal density fluctuations in supercritical CO_2 give rise to scattering of neutrons as described by the Ornstein-Zernike (OZ) law in Eq. (1). The

$$d\Sigma/d\Omega(Q) = d\Sigma/d\Omega(0)/[1 + (\xi Q)^2] \tag{1}$$

differential macroscopic cross section $d\Sigma/d\Omega(Q)$ represents the scattered intensity per unit volume in units of cm^{-1}. It is measured as a function of the modulus of scattering vector Q determined as $|Q| = (4\pi/\lambda)\sin(\delta/2)$ from the neutron wavelength λ and the scattering angle δ. $d\Sigma/d\Omega(Q)$ delivers two parameters, namely, $d\Sigma/d\Omega(0)$ and the correlation length ξ of thermal fluctuations. The structure facture factor $S(Q)$ is connected to $d\Sigma/d\Omega(Q)$ via $S(Q) = d\Sigma/d\Omega(Q)/K$, with the contrast factor $K = n(P) \times [b_{CO_2}]^2$ describing the interaction of neutrons and the atoms of CO_2 [16]. The present experiment was performed at constant volume V and temperature T, which means that the scattering of neutrons is caused by CO_2 number density fluctuations.

The structure factor at $Q = 0$, i.e., $S(Q = 0)$, is a susceptibility for which molecular gases and fluids are determined according to Eq. (2) by the mean square

$$S(0) = \langle \Delta N^2 \rangle / \langle N \rangle = k_B T \left. \frac{\partial n}{\partial P} \right|_{T,V}, \tag{2}$$

deviation of molecular number N as well as the product of the Boltzmann constant k_B, absolute temperature T, and first derivative of the number density $n(P)(= \langle N \rangle / V)$ with respect to P. Equation (2) represents a fluctuation dissipation theorem as outlined in [14] (pp. 103 and 337). This means that $S(0)$ can be evaluated on basis of the isothermal number density $n(P)$ known from the equation of state determination, such as found in [17].

At larger pressure fields, we observe the formation of larger scattering units, which will be analyzed with the scattering law of Eq. (3) formulated as a combination of

$$\frac{d\Sigma}{d\Omega}(Q) = \frac{d\Sigma}{d\Omega}(0)\exp(-u^2/3) + P_4\{[\mathrm{erf}(u/\sqrt{6})]^3/Q\}^4 \tag{3}$$

Guinier and Porod laws [16], representing a convenient form analyzing a scattering pattern over a larger Q regime [18]. The parameter $u = R_g Q$ determines the radius of gyration R_g, whereas $d\Sigma/d\Omega(0) = \Phi V_D \Delta\rho^2$ and $P_4 = 2\pi S_D \Delta\rho^2$ represent the scattering at $Q = 0$ and the Porod constant in the case of a smooth particle surface, respectively. Both parameters determine the droplet volume fraction Φ, volume V_D, and total surface S_D per unit volume. The scattering contrast $\Delta\rho^2$ is determined from the difference of the coherent scattering length densities of the droplet D and supercritical fluid F, i.e., $\Delta\rho = [\rho_D - \rho_F]$ [15]. For CO_2, one has $\rho_{D,F} = n_{D,F} \times b_{CO_2}$ ($n_{D,F}$ number density of CO_2 in phase D and F) and therefore the simplified expression $\Delta\rho = \rho_F[\Delta n/n_F]$.

SANS data.—CO_2 was measured at constant temperature (45 °C) and external pressure fields between 60 and 460 bar. Figure 2(a) shows the scattering data in Zimm representation measured at short sample-to-detector distance. The data at and below 120 bar follow the Ornstein-Zernike law (2) over the whole Q range, delivering the extrapolated scattering cross section at $Q = 0$ $[d\Sigma/d\Omega(0)]$ and the correlation length ξ of thermal density fluctuations. At 150 bar and beyond, we observe at low Q a continuously increasingly deviation from the OZ law, indicating formation of new scattering centers of larger size. In Fig. 2(b), these data are complemented with data obtained at larger sample-to-detector distance, i.e., smaller Q. The data were fitted with Eq. (3), considering the scattering from thermal fluctuations depicted as dashed-dotted lines. The

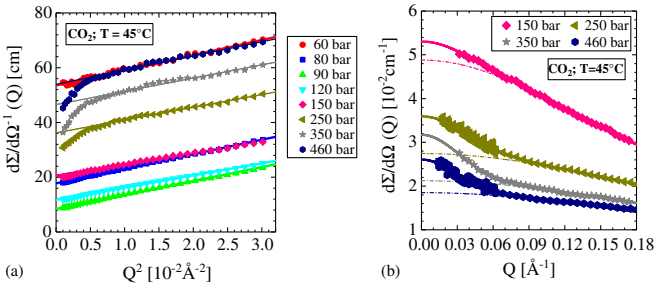

FIG. 2. Scattering data in (a) Zimm and (b) linear representation. The Zimm plot shows data from all pressure fields. At 120 bar and below the data are following straight lines, as expected from thermal fluctuation. Beyond 120 bar, strong deviation from the straight lines is observed. These data, together with two data sets measured at larger detector-to-sample distance, are depicted in (b) showing formation of droplets.

corresponding fits shown by the solid lines well describe the scattering data.

Data analysis.—The parameters of the OZ fits are depicted in Fig. 3(a), showing the extrapolated scattering cross section $d\Sigma/d\Omega(0)$ and correlation length ξ (see also Supplemental Material Table SI [7]). Both parameters show a distinct peak near 90 bar, indicating the nearby Widom line. The solid line in Fig. 3(a) represents $d\Sigma/d\Omega(0)$ evaluated on the basis of Eq. (2) from the first derivative of $n(P)$ with respect to the pressure P $(\partial n/\partial P|_{V,T})$ and parameters in Table SII.

The number density $n(P)$ was derived from the isothermal (45 °C) mass density taken from [17] and plotted together with $\partial n/\partial P|_{V,T}$ as solid lines in Fig. 3(b), determining the Widom line at 99.5 bar. Both values of $d\Sigma/d\Omega(0)$ were independently determined, showing

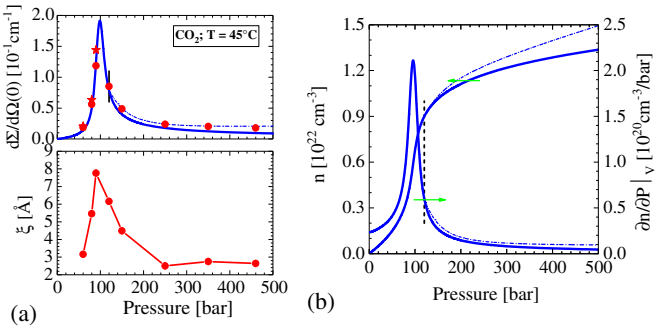

FIG. 3. Susceptibility and correlation length of thermal density fluctuations. (a) The data with solid circles and stars were measured at 1.70 and 7.70 m detector-to-sample distances, respectively. The solid line describing the susceptibility was evaluated on the basis of the number density $n(P)$ depicted in (b) and determined from equation of state theory. The maximum of $\partial n/\partial P|_{V,T}$ and $d\Sigma/d\Omega(0)$ of both figures represent the Widom line at 45 °C. The dash-dotted lines represent corrections of $n(P)$ above 120 bar on the basis of the SANS data, indicating a larger number density. The vertical lines at 120 bar in (a) and (b) represent the Frenkel line at 45 °C.

excellent quantitative agreement in the lower pressure regime. However, beyond 120 bar, a larger "SANS" susceptibility between 23% and 88% is measured if compared with the "equation-of-state" values and which corresponds to an enhanced CO_2 density of about 10% at $P = 460$ bar (Supplemental Material Table SII). The enhanced densification of supercritical CO_2 is accompanied by formation of larger scattering centers, which we interpret as droplets. As the SANS susceptibility was determined from the OZ law at $Q > 0.08$ Å^{-1} [Fig. 2(a)], the larger $\partial n/\partial P|_{T,V}$ and thereby $n(P)$ corresponds to the supercritical fluid. Both numbers are depicted as dashed-dotted lines in Figs. 3(a) and 3(b), the first one describing correctly the experimental SANS susceptibility. It has to be mentioned that the SANS susceptibilities indicated by the star symbol in Fig. 3(a) were measured at smaller Q after having finished all the "large" Q experiments (solid circles) demonstrating dissolution of the CO_2 droplets when passing back into the gaslike region.

The corresponding fit parameters of the droplets, such as radius of gyration R_g and extrapolated forward scattering $[d\Sigma/d\Omega(0)]$, are plotted in. 4(a) and 4(b) versus pressure and mass density, as well as compiled in Supplemental Material Table SIII. The size of the droplets only slightly increases from about 35 to 44 Å, whereas the correlation length declines from about 4.5 to 3.1 Å similar to the susceptibility when removed from the Widom line. The triangle in Fig. 4 represents R_g determined from the ratio of $d\Sigma/d\Omega(0)$ and the second moment of the scattered intensity $Q2$ [Supplemental Material Eq. (S-2) and Tables SIII and SIV] confirming the determined ones (solid circles) on the basis of Guinier's law (4).

The scattering from the droplets at $Q = 0$ depends on their volume and volume fraction, as well as on scattering contrast, as outlined in the theoretical part. The dashed line

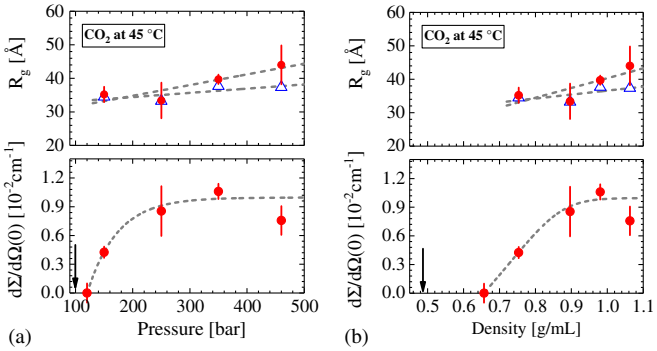

FIG. 4. Radius of gyration and scattering intensity at $Q = 0$ of the droplets versus pressure (a) and density (b). R_g indicated by Δ was determined from the ratio of $d\Sigma/d\Omega(0)$ and $Q2$ (see Tables SIII and SIV in the Supplemental Material). The fit of $d\Sigma/d\Omega(0)$ with an exponential (dashed line) is a guide for the eye, showing constant values above 250 bar. The zero intensity at 120 bar corresponds to a density of 0.658 g/mL. The arrow shows the position of the Widom line at 99.5 bar and 0.487 g/mL.

in the lower part of Fig. 4 represents an exponential fit serving as guide for the eye; it starts at 120 bar and becomes fairly constant beyond 250 bar. As the droplets are rather constant in size, the increase of droplet scattering is mainly determined from the product of droplet volume fraction Φ_D and scattering contrast $\Delta\rho^2$. The second moment $Q2$ in Supplemental Material Table SIII allows evaluation of droplet volume fraction Φ_D in the case of known number densities of both phases [Supplemental Material Eq. (S-2)]. In the present case, we do not know $n_D(P)$ nor the volume fraction Φ_D of the droplets. According to Eq. (S-2) we can only give a relationship between Φ_D and the absolute value of $n_L(P)$ according to $\Phi_D = A/[\Delta n/n_F]^2$ with $\Delta n = (n_D - n_F)$ and $A{:=}Q2/(2\pi^2\rho_F^2)$, assuming a small Φ_D. For a 10% difference of n_D with respect to n_F, and considering the parameter A in Supplemental Material Table SIV, we evaluate an average droplet volume fraction of 0.4%.

Summary and discussion.—The essential result of the present SANS experiment is the observation of a phase transition at a pressure field slightly above the Widom line. The change of phase appears as a formation of low concentration droplets of about 100 Å diameter and a 10% increase of particle number density of the supercritical fluid at 460 bar if compared with the predicted one from equation of state theories [17]. We interpret this phase boundary as the Frenkel line.

Recent experimental studies confirm structural changes in supercritical fluids. Acoustic waves combined with MD simulation and inelastic x-ray scattering in supercritical argon shows sharply enhanced positive dispersion when crossing a line identified as the Widom line [5]. Another study determined interatomic distances of supercritical argon performing x-ray diffraction in a Q range from 1 to 6.5 $Å^{-1}$ [19]. A continuous change of molecular distance was reported when passing the Frenkel line. A pathway along the Frenkel line was chosen, first in the liquidlike regime and then after passing the Frenkel line in the gaslike regime. In this way, a stronger variation of the position of interference peak was detected in the gaslike regime, thereby indicating different molecular densities on both sides of the Frenkel line. Such structural change confirms our observation of enhanced CO_2 number density when passing the Frenkel line [19,20]. To our knowledge, droplet formation was not observed before. Both mentioned experiments are not sensitive to larger objects because their experiments were performed at too large Q on the order of ~ 1 $Å^{-1}$.

Several MD simulations were undertaken to determine the Frenkel line of supercritical CO_2, as depicted in the phase diagram (Fig. 1) [4,8,10]. The Frenkel line by Fomin *et al.* has been determined on the basis of isochoric heat capacity (see Figs. 4 and 8 in [8]) and is depicted with solid squares and circles. These data differ from the Frenkel line determined by Yang *et al.* [10] (solid triangle) using the velocity autocorrelation function as the criterion; their Frenkel line already starts at $0.7–0.8T_C$ at P_C, showing a similar slope as the former one, but shifted to about 160 K lower temperature. The third Frenkel line (dashed-dotted line) was evaluated for a Lennard-Jones fluid and taken from Fig. 18(a) in [4]; it crosses 45 °C at about 138 bar, very near to the SANS value. A Frenkel line of supercritical CO_2 was also determined by Bolmatov *et al.* on the basis of the speed of sound, as shown in Figs. 5 and 6 in [20], showing a similar shape as the Widom line, but shifted to slightly larger temperature.

A comparison of the Frenkel lines in Fig. 1 shows that MD simulations deliver very uncertain results, which seem to strongly depend on the criterion used. This situation particularly underlines the relevance of experimental proof such as performed in the present Letter. This experiment, however, can only be a first step. More SANS experiments are necessary in order to determine the Widom and Frenkel lines at several temperatures beyond T_C. Those experiments are demanding, as the Frenkel line represents a borderline of continuous structural transition, as shown for the droplet formation in Fig. 4. Narrow pressure steps in combination with good statistical accuracy of the SANS data are needed in the region of the Widom line and structural transition. Such data may help to find a proper criterion for MD simulation, as well as clarify the relationship between the lines named after B. Widom and J. Frenkel.

We would like to thank Herbert Feilbach for development of the pressure cell, and Daniel Vujevic, Georg Brandl, and Alexander Weber for design and integration of the high-pressure setup. D. S. would like to thank Professor Winfried Petry from the Physik-Department at TUM for his support and Professor Stephan Förster from FZ-Jülich (Germany) for his hospitality. The experiments of this work were performed at the KWS 1 instrument operated by JCNS at the Heinz Maier-Leibnitz Zentrum (MLZ) Garching (Germany).

*Corresponding author.
d.schwahn@fz-juelich.de

[1] T. Wu and B. Han, in *Innovations of Green Chemistry, and Green Engineering*, edited by P. T. Anastas and J. B. Zimmerman (Springer Science and Business Media, New York, 2013).

[2] G. D. Wignall, in *Computational Studies, Nanotechnology, and Solution Thermodynamics of Polymer Systems*, edited by M. Dadmun *et al.* (Kluwer Academic, New York, 2000).

[3] A. Imre, C. Ramboz, T. Kraska, and U. K. Deiters, Environ. Earth Sci. **73**, 4373 (2015).

[4] V. V. Brazhkin, A. G. Lyapin, V. N. Ryzhov, K. Trachewnko, Yu. D. Fomin, and E. N. Tsiok, Phys. Usp. **55**, 1061 (2012).

[5] G. G. Simeoni, T. Bryk, F. A. Gorelli, M. Krisch, G. Ruocco, M. Santoro, and T. Scopigno, Nat. Phys. **6**, 503 (2010).

[6] P. F. McMillan and H. E. Stanley, Nat. Phys. **6**, 479 (2010).

[7] See Supplemental Material at http://link.aps.org/supplemental/10.1103/PhysRevLett.120.145701 for parameters of the CO_2 molecule, the susceptibility and correlation length of thermal density fluctuations of supercritical CO_2 as well as parameters of the droplet phase together with the number density of the densified supercritical CO_2 are compiled in four Tables. Furthermore, the equation of the Widom line on basis of the compressibility is given.

[8] Yu. D. Fomin, V. N. Ryzhov, E. N. Tsiok, and V. V. Brazhkin, Phys. Rev. E **91**, 022111 (2015).

[9] J. Frenkel, in *Kinetic Theory of Liquids*, edited by R. H. Fowler, P. Kapitza, and N. F. Mott (Oxford University Press, New York, 1947), p. 188.

[10] C. Yang, V. V. Brazhkin, M. T. Dove, and K. Trachenko, Phys. Rev. E **91**, 012112 (2015).

[11] M. E. Fisher and B. Widom, J. Chem. Phys. **50**, 3756 (1969).

[12] M. E. Fisher, *Excursions in the Land of Statistical Physics* (World Scientific Publishing Co., Singapore, 2017).

[13] https://fzj.frm2.tum.de/.

[14] R. K. Pathria and P. D. Beale, *Statistical Mechanics*, 3rd ed. (Elsevier, Amsterdam, 2011).

[15] V. F. Sears, Neutron News **3**, 26 (1992).

[16] R. J. Roe, *Methods of X-Ray and Neutron Scattering in Polymer Science* (University Press, Oxford, 2000).

[17] E. W. Lemmon, M. O. McLinden, and D. G. Friend, in *NIST Chemistry Webbook, NIST 69 Standard Reference Database*, edited by P. J. Linstrom and W. G. Mallard (NIST, Gaithersburg, MD), Vol. 20899, http://webbook.nist.gov/chemistry/fluid/ (retrieved October 2017).

[18] G. Beaucage, J. Appl. Crystallogr. **28**, 717 (1995).

[19] D. Bolmatov, M. Zhernenkov, D. Zav'yalov, S. N. Tkachev, A. Cunsolo, and Y. Q. Cai, Sci. Rep. **5**, 15850 (2015).

[20] D. Bolmatov, D. Zav'yalov, M. Gao, and M. Zhernenkov, J. Phys. Chem. Lett. **5**, 2785 (2014).